

Sequential Radiochemical Procedure for Isotopic Analysis of Uranium and Thorium in Egyptian Monazite

W. M. Abdellah*

Egypt Nuclear and Radiological Regulatory Authority, P.O. Box 7551, Cairo, Egypt

**e-mail: wmsra@yahoo.com*

Received August 27, 2018; revised December 26, 2018; accepted December 28, 2018

Abstract—Gamma and alpha spectrometry techniques were applied to determine the activity concentrations of ^{238}U and ^{232}Th (Bq kg^{-1}) as well as the $^{234}\text{U}/^{238}\text{U}$ and $^{230}\text{Th}/^{234}\text{U}$ isotopic ratios for commercial grade monazite (purity ~50%) supplied from the Egypt nuclear materials authority. A method for total dissolution of monazite followed by the sequential radiochemical separation using anion-exchange chromatography is presented. The average activity concentrations of ^{238}U and ^{232}Th , measured by α -ray spectrometry, are 2.49 g kg^{-1} (0.24 wt %) and 30.09 g kg^{-1} (3.1 wt %), respectively. The calculated $^{234}\text{U}/^{238}\text{U}$ and $^{230}\text{Th}/^{234}\text{U}$ isotopic ratios are close to unity, suggesting closed system equilibrium. The possibility of using leaching of monazite with water at different pH values for gaining information about the masses of uranium and thorium that pass into the solution and remain fixed in the crystal lattice was examined.

Keywords: black sand, monazite, leaching, uranium, thorium, isotopic ratio, Egypt

DOI: 10.1134/S1066362219040118

INTRODUCTION

Beach sand mineral is a term generally used to define beach deposits of zircon, ilmenite, granite, rutile, and other accessory minerals. On the other hand, monazite is one of the most important geological materials containing uranium and thorium, which are the main elements used as nuclear fuel [1]. The separation of the raw sands was done previously by the method of specific gravity after removing the light sand with clay. In recent years, heavy sand mineral concentrates became a subject of active studies. The separation of valuable heavy sand minerals into individuals is based on particle size, electrical conductivity, and magnetic susceptibility of heavy minerals [1]. Monazite is a natural phosphate mineral containing several rare earth and actinide elements, mainly thorium, cerium, and lanthanum. All these metals are used in industry and are considered valuable. Zircon and zircon sand are also used in industry as fireproof materials, abrasives, electronics, construction materials, and nuclear industrial materials. However, high thorium and uranium content of monazite may cause unexpected radiation exposure of workers and members of the public [2]. In the last decade monazite ore has attracted much attention from Egyptian research teams because of the high

content of some valuable heavy metals and rare earth elements, which can be used both in local industries and scientific research.

Egyptian monazite ore was obtained by the Nuclear Material Authority of Egypt from black beach sand of Abou-Kashaba deposit near Rosetta, extending from Rosetta to Rafah city through 400 km. Sroor [3] studied the activity concentration of natural radionuclides in monazite samples and showed that the ^{238}U content varied from 53 to 61 kBq kg^{-1} , ^{232}Th content, from 205 to 232 kBq kg^{-1} , and ^{40}K content, from 15 to 20 kBq kg^{-1} [3]. El-Afifi [4] shows that the average activity concentrations of ^{238}U , ^{232}Th , and ^{40}K in Egyptian black sand were 260 ± 25 , 410 ± 43 , and $330 \pm 30 \text{ Bq kg}^{-1}$, respectively. The concentrations fluctuated depending on the sampling site [3, 4].

In this study, the radionuclide concentrations were determined in commercial-grade Egyptian monazite samples (purity ~50%) separated from local beach near Rosetta (Abou-Khashaba), Egypt. The γ - and α -ray spectrometric analyses were applied to determine the ^{238}U and ^{232}Th activity concentrations (Bq kg^{-1}). The sequential radiochemical procedure for isotopic analysis of uranium and thorium was applied to determine the $^{234}\text{U}/^{238}\text{U}$ and $^{230}\text{Th}/^{234}\text{U}$ isotopic ratios.

EXPERIMENTAL

Materials and chemicals. Four monazite ore samples were provided by the Egyptian Nuclear Material Authority. Figure 1 shows the location of the main black sand deposits. The extraction procedure, performed according to [5, 6], is shown in Fig. 2. The samples were ground, sieved to 200 mesh, and prepared for analysis. DL-1a material (Canada Center for Mineral and Energy Technology, Ottawa, Ontario) was used in the study as a certified reference material for uranium and thorium. All the chemicals and solvents used were of analytical reagent and spectroscopic grade. Water was deionized and purified using the Milli-Q system (resistivity 18.2 MΩ cm). All laboratory dishes (beakers, bottles) used in this study were made of Teflon. Highly pure grade acids HCl, HNO₃, and HF and Dowex 1×4 ion exchange resin (Cl⁻ form, 50–100 mesh, Fluka) were used. The chemical yield was determined using ²³⁶U and ²²⁹Th tracers.

Chemical and petrographic analysis. Picked mineral grains representing different varieties of both monazite and other minerals (impurities) were investigated using a JXA-8600 scanning electron microscope (SEM) equipped with an electron probe microanalyzer (EPMA). The SEM energy-dispersive X-ray (EDAX) analyses were made to determine and quantify the chemical composition of the samples.

The petrographic study of the samples was aimed at determining the mineral phases present in the sample and was made using EPMA. The analyzed spots mainly cover the core and rims of grains of monazite and other impurities. These analyses were carried out at the University of Helsinki, Finland.

γ-Ray spectrometric analysis. A γ-ray spectrometer equipped with a hyperpure germanium (HP-Ge) detector was used. The spectrometer consists of a detector of vertical configuration mounted on a 30-L liquid nitrogen Dewar tank for the temperature control of the germanium crystal. Canberra DSA-1000 desktop spectrum analyzer was used.

The spectrometer was energy calibrated using a ¹⁵²Eu source. The efficiency calibration was done using multi-nuclide standard solution no. 7503 (Eckert & Ziegler) containing ²¹⁰Pb, ²⁴¹Am, ¹⁰⁹Cd, ⁵⁷Co, ^{123m}Te, ⁵¹Cr, ¹¹³Sn, ⁸⁵Sr, ¹³⁷Cs, ⁸⁸Y, and ⁶⁰Co. The measuring geometry used in this study was 15 mL of the sample in a 20-mL Packard liquid scintillation polyethylene vial. The HP-Ge detector had a relative efficiency of

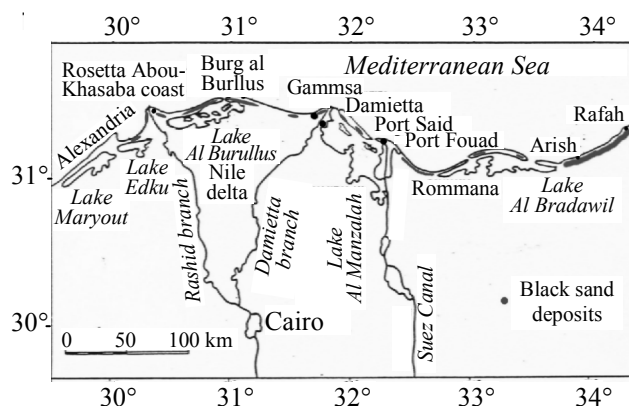


Fig. 1. Nile delta map showing locations of the main black sand deposits.

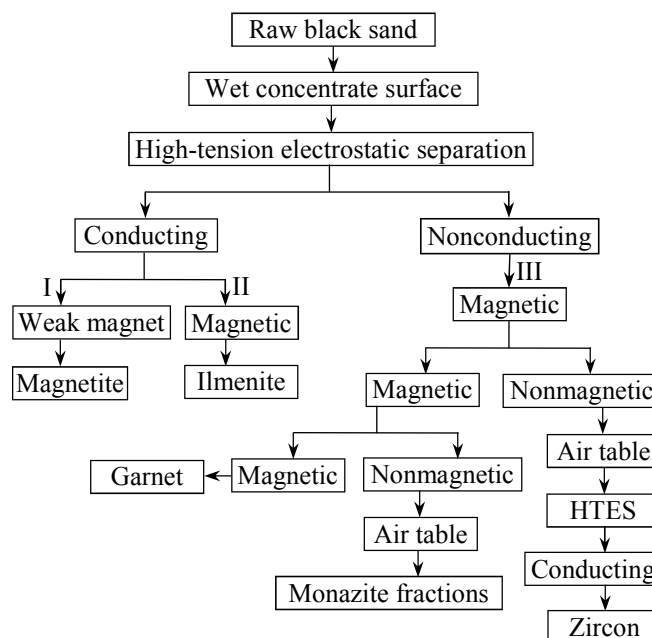


Fig. 2. Flowchart of minerals extraction process from black sand [5, 6].

45% and full width at half-maximum (FWHM) of 1.95 keV for the ⁶⁰Co γ-line at 1332 keV. The device was operated with Canberra Genie 2000 software for gamma acquisition and analysis.

The γ-rays emitted naturally from monazite samples are mainly due to the daughters of ²³⁸U and ²³²Th series. The energies are 62.9 and 92.8 keV for ²³⁴Th, 241.9 and 351.9 keV for ²¹⁴Pb, 609.3 and 2204.2 keV for ²¹⁴Bi (all ²³⁸U series), 185.7 keV for ²³⁵U [7], and 270.2, 338.2, 911.2, and 968.9 keV for ²²⁸Ac (²³²Th series).

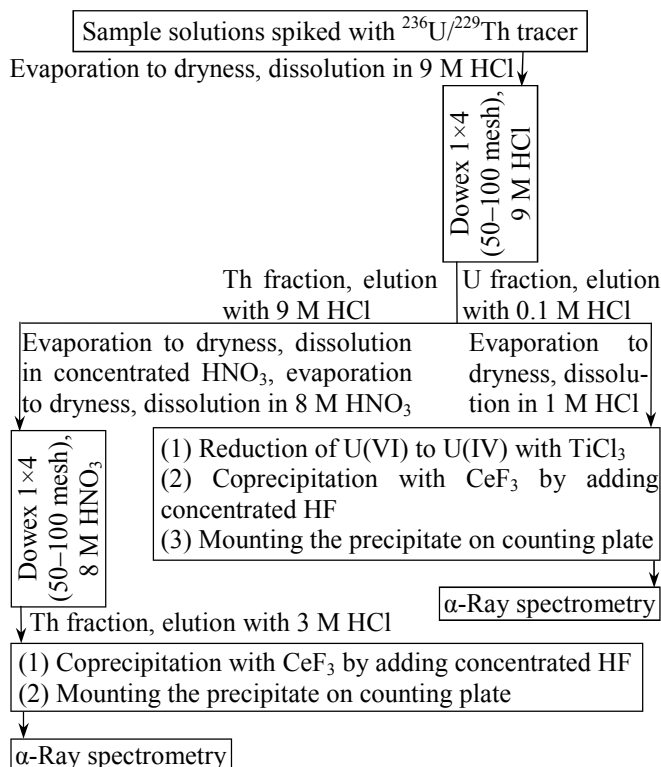


Fig. 3. Schematic diagram for sequential analysis of U/Th isotopes in the sample.

In this study, ^{238}U was identified by the γ -ray peak at 1001 keV for ^{234m}Pa . This line has low intensity but is clearly manifested in the spectra. The ^{232}Th identification is based on the ^{228}Ac γ -ray peaks at 911.60, 964.60, and 969.11 keV. The activity concentration of ^{40}K was measured by its own γ -line at 1460.8 keV [8, 9]. These peaks were selected to avoid interference with other peaks in the γ -ray spectra.

α -Ray spectrometric analysis. α -Ray spectrometry was used for determining the concentrations of uranium and thorium isotopes after sequential radiochemical separation. The spectrometers were equipped with PIPS detectors of 450 mm² area with the efficiency ranging from 17 to 25%; the detectors were connected to a computerized multichannel analyzer operating with Maestro software (ORTEC). The samples were measured for no less than 60000 s; the minimum detectable activity (MDA) was 1 mBq. The technique is described in detail in [10].

Sequential analysis for uranium/thorium isotopes. *Decomposition of monazite ore.* Concentrated acids HNO_3 , HF , and HCl (4 mL each) were added to 50 mg of commercial grade monazite ore (purity 50%,

50–100 mesh). The tubes with the mixtures were put into a Mars CEM microwave oven. The experiments were performed at pressures of up to 160 psi and temperature of up to 190°C. Model XP 1500 were used. After the pressure reached less than 50 psi and the temperature, less than 50°C, the samples were taken off and evaporated to dryness. The residues were mixed with concentrated perchloric and nitric acids and evaporated to dryness; finally, the samples were dissolved in hydrochloric acid and filtered.

Radiochemical separation. The samples were spiked with ^{236}U and ^{229}Th with the activities of 1.40 and 12.00 DPM g⁻¹, respectively. The separation was carried out using Dowex 1×4 anion exchange resin (50–100 mesh). The sequential radiochemical separation of U/Th isotopes followed the diagram shown in Fig. 3. The ion-exchange column is pretreated with 9 M HCl, and the sample solution is loaded into the column. Uranium is retained on the resin, whereas thorium passes through the column. Uranium is eluted from the column with 0.1 M HCl; at this concentration, the uranium chloride complexes are broken down. The thorium-containing eluate is evaporated to dryness, dissolved in 8 M HNO_3 , and poured onto an anion-exchange column in which thorium is retained as a nitrate complex. The thorium fraction is then eluted from the column with dilute HCl. Finally, the separated uranium and thorium are coprecipitated with CeF_3 , and the precipitate is filtered off using a 0.1- μm filter paper before counting using α -ray spectrometry. The procedure was studied and validated previously [11, 12]. The analytical quality control measurements were regularly performed through the certified reference material (DL-1a) and blank analyses. The results obtained are reported and evaluated taking into consideration the counting statistics and tracer activity error.

Monazite–water interactions. Five steps were considered in the sequential procedure to extract uranium and thorium from monazite (leaching experiments). The leaching experiment was applied because the Rosetta area is located above the aquifer which may be contaminated as a result of monazite–water interactions. We studied the interaction of monazite with water acidified with HCl to simulate seawater rich in chloride ions [13]. The leaching solutions [tap water, distilled water at pH 7, 6, and 4 to simulate acid rains, and acidified water (1 M HCl)] were taken to evaluate the masses of uranium and thorium isotopes

that may be released from monazite into the environment.

The sample weight in leaching experiments was 5 g, and the volume of each leaching solution was 20 mL. The experiments were performed using centrifuge tubes with stirring overnight, and the solid and liquid phases were separated by centrifugation and filtration through a 0.45- μm Millipore filter. The interaction between monazite and leaching solutions was continuously monitored throughout the process. After each leaching step, the solution was divided into two parts to perform α -ray spectrometric and ICP-MS analyses.

RESULTS AND DISCUSSION

Chemical and petrographic analysis. The results of preliminary analysis of monazite by energy-dispersive spectrometry (EDS) supported with electron microprobe are shown Fig. 4a for the uncoated grains on carbon tape. They show slight charging. The backscattered electron (BSE) detector images of the grain with high contrast settings reveals at least two major phases (Fig. 4b): monazite (two bright grains) and zircon (two grains analyzed). The SEM images in combination with EDS spectra are shown in Figs. 5a and 5b for monazite-Ce (test grain nos. 1 and 2) and in Figs. 5c and 5d for zircon (the test grain nos. 3 and 4). The concentrations of zircon and monazite minerals in the ore show wide spatial variations. The differences are essentially due to paramagnetic character of the upstream rocks. The grains also differ in shape and size. Zircon grains are elongated, whereas monazite grains are well rounded (Fig. 5), in agreement with the previous data [14, 15]. Table 1 summarizes the elemental composition and SEM/EDS spectra for the entire area in the images shown in Fig. 5.

The quantitative analysis using both backscattered electron images and electron probe microanalysis (EPMA) shows that monazite is present in the cerium form (monazite-Ce): The Ce content varied from 13.5 to 16.9% (Table 1). These results are in good agreement with the previous data [16, 17]. Grain nos. 1 and 2 contain the following elements: O, F, Si, P, Ca, La, Ce, Nd, Pb, Th, and U. The monazite samples are richer in O, Ce, and P and leaner in Sm and Al. The chemical analysis of the samples furnishes important information about the distribution of U and Th in the monazite samples without measuring isotopic ratios [18]. The quantitative analysis using electron microprobe shows that the monazite ore is enriched in Th

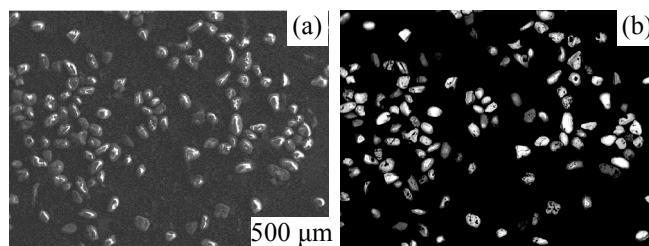


Fig. 4. (a) Secondary electron (SE) image of the uncoated grains on carbon tape and (b) backscattered electron (BSE) image of the grain mount with high contrast settings.

(5.02–5.19 wt %) rather than in U (1.02–1.24 wt %). The quantitative elemental analysis for zircon grains (nos. 3 and 4) showed high content of O (55.7–56.2 wt %), Zr (30.87–32.30 wt %), and Si (11.25–13.10 wt %) and lower content of Al (0.32–0.33 wt %).

Activity determination by gamma spectrometry. The activity is calculated from the count rate for each energy and the intensity of each line, considering the sample mass, branching ratios of γ -decay, counting time, and detector efficiency. Table 2 presents the activity concentrations for primordial radionuclides in monazite. They range from 45.1 ± 1.7 to 49.0 ± 2.2 , from 81.0 ± 1.7 to 87.5 ± 1.5 , and from 9.29 ± 0.08 to 10.6 ± 1.1 Bq g^{-1} for ^{238}U , ^{232}Th , and ^{40}K , respectively. The average activity concentrations are 46.9 ± 1.8 , 83.1 ± 1.5 , and 10.0 ± 0.7 Bq g^{-1} for ^{238}U , ^{232}Th , and ^{40}K respectively. Comparison of the results obtained with the results of previous studies (Table 3) shows that the activity concentration of ^{238}U , ^{232}Th , and ^{40}K vary in a wide range depending on the origin of the ore

Table 1. Quantitative EPMA analysis (wt %) of monazite and zircon grains

Monazite			Zircon		
element	grain 1	grain 2	element	grain 3	grain 4
O	40.65	46.37	O	55.70	56.2
F	4.78	5.17	Al	0.33	0.25
Al	0.35	0.43	Si	13.10	11.25
Si	1.32	1.11	Zr	30.87	32.3
P	13.11	14.46			
Ca	0.91	1.22			
La	9.32	7.07			
Ce	16.90	13.52			
Nd	5.18	3.38			
Sm	0.28	–			
Pb	0.98	1.03			
Th	5.19	5.02			
U	1.02	1.24			

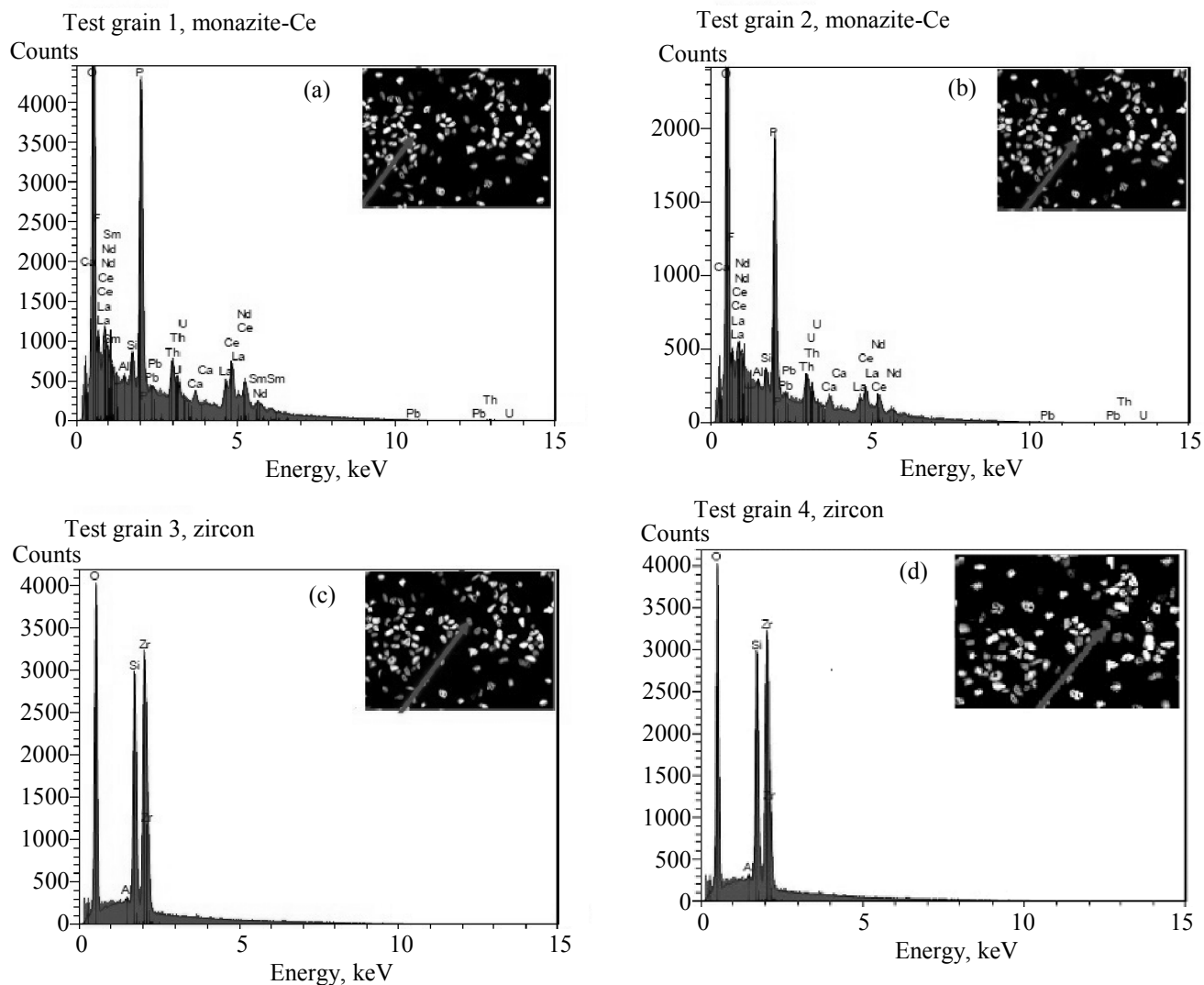


Fig. 5. SEM/EDS spectra for quantitative elemental analysis of the entire area in the images (a, b) for monazite grains (nos. 1 and 2) and (c, d) for zircon grains (nos. 3 and 4).

and the chemical composition. The results show that the monazite samples have relatively high activity concentrations of ^{238}U , and the radiological hazard for the workers dealing with the monazite ore during the extraction process should be taken into account. The radiation protection regulations recommended by IAEA and the national regulatory body should be applied [5].

Determination of U and Th isotopes by α -ray spectrometry. The results are summarized in Table 4. The ^{238}U concentration ranges from 2000 ± 76 to 2806 ± 97 ppm with an average 2483 ± 80 ppm, and the ^{232}Th concentration ranges from $25\,523 \pm 828$ to $34\,455 \pm 839$ ppm with an average of $30\,989 \pm 856$ ppm. The average chemical recovery is about

Table 2. Activity concentrations of ^{238}U , ^{232}Th and ^{40}K (Bq g^{-1}) in monazite samples, determined by γ -ray spectrometry

Sample	^{238}U	^{232}Th	^{40}K
Monazite 1 (41.88 g)	46.5 ± 1.6	81.4 ± 1.0	9.29 ± 0.08
Monazite 2 (41.57 g)	45.1 ± 1.7	82.6 ± 1.8	10.2 ± 0.6
Monazite 3 (41.50 g)	49.0 ± 2.2	87.5 ± 1.5	10.6 ± 1.1
Monazite 4 (41.51 g)	49.0 ± 1.7	81.0 ± 1.7	9.7 ± 0.8
Average	46.9 ± 1.8	83.1 ± 1.5	10.0 ± 0.7

Table 3. Comparison between the activity concentrations of monazite (Bq kg⁻¹ monazite) with those found in similar studies

Country	²³⁸ U	²²⁶ Ra	²³² Th	⁴⁰ K	References
Egypt	46 890 ± 1790 –	– 40 580 ± 1370	83 130 ± 1510 182 425 ± 9870	9950 ± 650 11 300 ± 9570	This work [4]
Australia	6000–30 000	–	40 000–2 500 000	–	[19]
Belgium	Around 1000	–	6000–10 000	–	[20]
Malaysia	1857 ± 9	–	10 287 ± 9	–	[21]
India	21 500 ± 270	–	305 000 ± 2000	–	[22]
Bangladesh (heavy fraction of black sand)	–	2582 ± 2050	4684 ± 680	639 ± 21	[1]
UNSCEAR 2000 data	6000–40 000	–	8000–300 000	–	[23]

Table 4. Uranium and thorium concentration and isotopic ratios in monazite ore (~50 g), determined by α-ray spectrometry

Sample no.	²³⁸ U, ppm	²³² Th, ppm	²³⁴ U/ ²³⁸ U	²³⁰ Th/ ²³⁴ U
Monazite 1	2806 ± 79	34 455 ± 839	0.95 ± 0.02	1.20 ± 0.06
Monazite 2	2000 ± 76	25 523 ± 828	1.02 ± 0.04	0.94 ± 0.06
Monazite 3	2643 ± 85	32 988 ± 900	0.98 ± 0.03	1.06 ± 0.06
DL-1a, experimental values	113 ± 2	73 ± 3	0.95 ± 0.017	1.08 ± 0.03
DL-1a (certified values and 95% confidence intervals), wt %	0.0116 ± 0.0003	0.0076 ± 0.0004		

Table 5. ²³⁸U and ²³²Th average concentration (ppb) in the liquid fractions after leaching 5 g of monazite ore

Extraction solution	²³⁸ U concentration	²³² Th concentration	²³⁴ U/ ²³⁸ U	²³⁰ Th/ ²³⁸ U
Tap water	1.97 ± 0.14	75 ± 7	0.94 ± 0.08	135 ± 13
Water pH ~ 7	0.33 ± 0.02	120 ± 6	1.04 ± 0.07	37 ± 3
Water pH ~ 6	0.64 ± 0.05	31 ± 3	0.57 ± 0.05	9.6 ± 1.2
Water pH ~ 4	60.9 ± 1.8	148 ± 6	1.07 ± 0.04	0.34 ± 0.02
HCl (1 M)	99.8 ± 2.4	4000 ± 84	1.07 ± 0.03	4.38 ± 0.16

80%. The activity concentrations in ppm were calculated using the following relationships [24]: 1 ppm Th = 4.06 Bq kg⁻¹ ²³²Th; 1 ppm U = 12.35 Bq kg⁻¹ ²³⁸U.

The calculated ²³⁴U/²³⁸U isotopic ratios for all the samples are close to unity, which corresponds to the closed system equilibrium (Table 4). The ²³⁰Th/²³⁴U ratios are slightly higher than unity for three samples. So, the examined crystals show no evidence for selective dissolution of uranium or thorium. The ratios below unity such as in sample no. 2 suggest some degree of dissolution, limiting the U migration during the alteration of uranyl oxide hydrates [25].

The calculated ²³⁰Th/²³⁴U ratios may be used for dating in the age range between 10 000 and 20 000 years; this time covers the most significant climatic changes according to [26].

Monazite–water interaction. The overall measurement results are summarized in Table 5. Uranium and thorium are distributed in crystalline rocks in three

main ways: (1) by direct cation substitution in the silicate lattice of the major rock-forming minerals; (2) as a minor or major component of accessory minerals such as zircon, apatite, and monazite; and (3) by sorption in rock pores, i.e., in lattice defects, microfissures, and grain boundaries [27].

Treatment with tap water removes the material sorbed in rock pores, in lattice defects, and on crystal grain boundaries [28]. The average concentration of ²³⁸U and ²³²Th in the tap water as a leaching solution is 1.97 ± 0.14 and 75 ± 7 ppb, respectively; these concentrations are attributed to rapid ion-exchange reactions. The measured concentrations in water at pH 7, 6, and 4 were 0.33 ± 0.02, 0.64 ± 0.05, and 60.9 ± 1.8 ppb for ²³⁸U and 120 ± 6, 31 ± 3, and 148 ± 6 ppb for ²³²Th, respectively. That is, the uranium and thorium concentrations in the leaching solutions increase with decreasing pH, which can be attributed to the displacing effect of H⁺ ions.

The obtained large variations in the activity ratios

from 0.57 ± 0.05 to 1.07 ± 0.04 for $^{234}\text{U}/^{238}\text{U}$ and from 0.34 ± 0.02 to 37 ± 3 for $^{230}\text{Th}/^{238}\text{U}$ are in good agreement with the data of Harmon and Rosholt [28], who reported that the percentage of extracted Th was higher than that of U, i.e., that the U/Th mass ratio was somewhat lower in sorbed phase than in bulk rock. During the leaching process, recoil ^{234}U may be released from the samples due to the change in the electron shell configuration caused by preceding decay process; it is probably in the more soluble valence state +6 [29], whereas ^{238}U in the sample phase, representing the original uranium, can be assumed to be in the less soluble valence state +4, like ^{230}Th .

Regulatory aspects. The Egyptian Nuclear and Radiological Regulatory Authority (ENRRA) continually develops regulations and guidelines in order to ensure safe handling of naturally occurring radioactive materials (NORM) according to law no. 7 of 2010 [30] and its executive regulation of 2011 [31]. These legislations do not provide details on the requirements and criteria that should be taken by the owner; thus, IAEA radiation protection regulations [32, 33] and WHO guidelines [34] are applied.

CONCLUSION

The results obtained show that commercial-grade Egyptian monazite of ~50% purity can be considered as a source of ^{232}Th (Th content about 5 wt %). The average $^{234}\text{U}/^{238}\text{U}$ and $^{230}\text{Th}/^{234}\text{U}$ isotopic ratios are close to unity, which corresponds to the closed system equilibrium. Sequential leaching technique gave insight into the mechanisms controlling the distribution of mobilized U and Th isotopes into the environment. Construction of a suitable licensed location for the reservation of the monazite ore to protect the public, environment, and the workers from the potential exposure and contamination hazards is recommended.

ACKNOWLEDGMENTS

The author acknowledges the contribution made to this study by the Helsinki University radiochemical laboratory, students, their teachers, as well as the support from Dr. Juhani Suksi and Prof. Jukka Lehto.

FUNDING

The study was funded by the ParOwn organization for scientific research (project no. 15326).

CONFLICT OF INTEREST

The author declares that he has no conflict of interest.

REFERENCES

1. Alam, M.N., Chowdhury, M.I., Kamal, M., et al., *J. Environ. Radioact.*, 1999, vol. 46, no. 2, pp. 243–250. DOI: 10.1016/S0265-931X(98)00143-X.
2. Chang, B.U., Koh, S.M., Kim, Y.J., et al., *J. Environ. Radioact.*, 2008, vol. 99, no. 3, pp. 455–460. DOI: 10.1016/j.jenvrad.2007.08.020.
3. Sroor, A., *Appl. Radiat. Isot.*, 2003, vol. 58, no. 2, pp. 281–285. DOI: 10.1016/S0969-8043(02)00256-7.
4. El Afifi, E.M., Hilal, M.A., Khalifa, S.M., and Aly, H.F., *Radiat. Meas.*, 2006, vol. 41, no. 5, pp. 627–633. DOI: 10.1016/j.radmeas.2005.09.014.
5. Shiren, M.L., Radiological hazards resulting from the extraction of mineral from black sand, *PhD Thesis*, Egypt: Menofia Univ., Faculty of Science, 2010.
6. Mohammad, I.M., in *The Fifth International Conf. on the Geology of Africa*, Assiut (Egypt), 2007, vol. 1, pp. 107–124.
7. Kieff, I. and Kostadinov, K., *J. Radioanal. Chem.*, 1981, vol. 63, no. 2, pp. 397–404.
8. Sengupta, A., Sankhe, R.H., and Natarajan, V., *J. Radioanal. Nucl. Chem.*, 2015, vol. 306, no. 2, pp. 401–406. DOI: 10.1007/s10967-015-4088-3.
9. Guidotti, L., Carini, F., Rossi, R., et al., *J. Environ. Radioact.*, 2015, vol. 142, pp. 36–44. DOI: 10.1016/j.jenvrad.2015.01.010.
10. Currie, L.A., *Anal. Chem.*, 1968, vol. 40, no. 3, pp. 586–593. DOI: 10.1021/ac60259a007.
11. Juhani, S., Natural uranium as a tracer in radionuclide geosphere transport studies, *Report Ser. in Radiochemistry*, Helsinki Univ., 2001, issue 16/2001.
12. Jukka, L. and Hou, X., *Chemistry and Analysis of Radionuclides, Laboratory Techniques and Methodology*, Wiley, 2010, pp. 69–71.
13. Ellen, R., Whit, J., Bessie, S., and Jack, G., *Rainwater Chemistry across the United States: Advisor Report*, Bereket Haileab, 2004.
14. Meleik, M.L., Fouad, K.M., Wassef, S.N., et al., *Egypt Econ. Geol.*, 1978, vol. 73, pp. 1738–1748.
15. Ammar, A.A., Wassef, S.N., Meleik, M.L., et al., *Int. J. Remote Sens.*, 1983, vol. 4, no. 4, pp. 739–754.
16. Eissa, E.A., Rofail, N.B., Ashmawy, L.S., and Hassan, A.M., *Czechoslov. J. Phys.*, 1999, vol. 49, pp. 323–329. DOI: 10.1007/s10582-999-0042-3.
17. Crespo, M.T., Del Villar, L.P., Jiménez, A., et al., *Appl. Radiat. Isot.*, 1996, vol. 47, nos. 9–10, pp. 927–931. DOI: 10.1016/S0969-8043(96)00089-9.

18. Kremling, K., *Nature*, 1983, vol. 303, pp. 225–227. DOI: 10.1038/303225a0.
19. Cooper, M.B., Naturally occurring radioactive materials (NORM) in Australian industries—review of current inventories and future generation, *ERS-006: Report Prepared for the Radiation Health and Safety Advisory Council*, 2005, pp. 1–40.
20. Vandenhove, H., *Int. Congr. Ser.*, 2002, vol. 1225, pp. 307–315. DOI: 10.1016/S0531-5131(01)00525-8.
21. Bahari, I., Mohsen, N., and Abdullah, P., *J. Environ. Radioact.*, 2007, vol. 95, nos. 2–3, pp. 161–170. DOI: 10.1016/j.jenvrad.2007.02.009.
22. Mohanty, A.K., Das, S.K., Van, K.V., et al., *J. Radioanal. Nucl. Chem.*, 2003, vol. 258, no. 2, pp. 383–389. DOI: 10.1023/A:1026202224700.
23. *UNSCEAR Report*, New York, 2000, vol. 1.
24. Guidelines for radioelement mapping using gamma ray spectrometry data, *IAEA-TECDOC-1363*, Vienna: IAEA, 2003, no. 1363.
25. Finch, R.J. and Ewing, R.C., *Mater. Res. Soc. Symp. Proc.*, 1992, vol. 257, pp. 465–472.
26. Eronen, M. and Olander, H., On the world ice ages and changing environments, *Report YJT-90-13*, Helsinki: Nuclear Waste Commission of Finnish Power Companies, 1990.
27. Cronan, C.S., Reiners, W.A., Reynolds, R.C., and Lang, G.E., *Science*, 1978, vol. 200, pp. 309–311.
28. Harmon, R.S. and Rosholt, N.J., *Uranium Series Disequilibrium: Applications to Environmental Problems*, Ivanovich, M. and Harmon, R.S., Eds., Oxford: Clarendon, 1982, pp. 145–164.
29. Adolf, J.P. and Roessler, K., *Radiochim. Acta*, 1991, vols. 52/53, pp. 269–274.
30. Law regulating nuclear and radiation activities, no. 7 for 2010, *Egypt. Gaz.*, March 30, 2010.
31. Executive regulation for the law no. 7 for 2010, *Egypt. Gaz.*, Oct. 26, 2011.
32. Occupational radiation protection, *Safety Standard Ser.*, Vienna: IAEA, 1999, no. RS-G-1.1.
33. Radiation protection and safety of radiation sources: Int. basic safety standards, *Safety Standard Ser.*, Vienna: IAEA, 2014, no. GSR, part 3.
34. *Guidelines for Drinking-Water Quality*, Geneva: WHO, 2008, 3rd ed., vol. 1, pp. 220–204.